

# Supporting Information for

## **High Broadband Light Transmission for Solar Fuels Production Using Dielectric Optical Waveguides in TiO<sub>2</sub> Nanocone Arrays**

Sisir Yalamanchili<sup>1†</sup>, Erik Verlage<sup>1†</sup>, Wen-Hui Cheng<sup>1†</sup>, Katherine T. Fountaine<sup>5</sup>, Philip R. Jahelka<sup>1</sup>, Paul A. Kempler<sup>2</sup>, Rebecca Saive<sup>1</sup>, Nathan S. Lewis<sup>2,4\*</sup>, and Harry A. Atwater<sup>1,3\*</sup>

<sup>1</sup>Division of Engineering and Applied Sciences, California Institute of Technology, Pasadena, CA 91125

<sup>2</sup>Division of Chemistry and Chemical Engineering, California Institute of Technology, Pasadena, CA 91125

<sup>3</sup>Kavli Nanoscience Institute, California Institute of Technology, Pasadena, CA 91125

<sup>4</sup>Beckman Institute, California Institute of Technology, Pasadena, CA 91125

<sup>5</sup>NGNext, Northrop Grumman Aerospace Systems, Redondo Beach, CA 90278

<sup>†</sup>These authors contributed equally

\*Corresponding Authors: [haa@caltech.edu](mailto:haa@caltech.edu), [nslewis@caltech.edu](mailto:nslewis@caltech.edu)

## Methods

### *Simulation Methodology*

3D full-field electromagnetic wave finite-difference time-domain (FDTD) simulations of TiO<sub>2</sub> nanocone arrays with or without Ni films, with hexagonal arrays of holes on Si, were performed using a commercial software package, Lumerical FDTD. The nanocone arrays on Si were constructed using the 3D simulation region with periodic boundary conditions along the *x*- and *y*-axes, and infinite boundary conditions were rendered as perfectly matched layers along the *z*-axis. Palik materials data were used for Si and Ni. Material data from the Ioffe Institute and ellipsometry measurements were both used for simulation of the optical properties of the TiO<sub>2</sub> nanocones. A plane-wave source of illumination was applied to simulate the steady-state behavior of TiO<sub>2</sub> nanocones with or without Ni arrays on the Si substrate. Broadband simulations were performed in the 400 – 1100 nm spectral range for two orthogonal polarizations. Transmission spectra for unpolarized light were obtained by averaging the transmission spectra for the two orthogonal polarizations. These transmission spectra, along with the standard AM 1.5G spectra, were used to calculate the fraction of the spectral photon flux that was transmitted into the Si. The expected light-limited photocurrent density ( $J_{ph,max}$ ) can be estimated by integration of the transmitted spectral photon flux with the corresponding wavelength. Frequency-domain field and power monitors were applied in the simulation to produce the steady-state electric-field data for plots of electric-field profiles.

## *Fabrication procedure for p<sup>+</sup>n Si photoanodes with TiO<sub>2</sub> nanocones and Ni*

Czochralski-grown n-type Si wafers with <100> orientation and a resistivity of 0.1-1 ohm-cm (Addison Engineering Inc.) were cleaned via a modified RCA standard clean 1 (5:1:1 by volume of H<sub>2</sub>O:NH<sub>4</sub>OH:H<sub>2</sub>O<sub>2</sub> at 70 °C), then 1 min immersions in 10% (v/v) HF, and followed by an RCA standard clean 2 (6:1:1 H<sub>2</sub>O:HCl:H<sub>2</sub>O<sub>2</sub> (v/v) at 70 °C). The cleaned n-Si samples were thermally doped with boron using a BN-975 (Saint-Gobain) wafer at 950 °C for 30 min to produce a p<sup>+</sup>n-Si homojunction. The doped p<sup>+</sup>n-Si samples were immersed in 10% (v/v) HF(aq) for 2 min, oxidized in a tube furnace at 750 °C for 20 min, and then dipped in 10% (v/v) HF for 2 min, to remove any defective layers on the Si surface. A layer of SiO<sub>2</sub>(5 – 10 nm) was deposited onto the p<sup>+</sup>n Si wafers via electron-beam evaporation, and 2.3 μm of TiO<sub>2</sub> was then deposited onto the samples via electron-beam evaporation. Electron-beam evaporation depletes the source of oxygen and results in TiO<sub>2</sub> with higher conductivity than perfectly stoichiometric TiO<sub>2</sub>, so the deposition was performed in 3-4 steps, refilling the TiO<sub>2</sub> source between steps to maintain higher oxygen content in the film. The TiO<sub>2</sub>-coated p<sup>+</sup>n-Si samples were spin-coated at 4000 rpm for 60 s with 495 PMMA A4 and baked at 80 °C for 5 min, and then spin-coated at 4000 rpm for 60 s with 950 PMMA A4 and baked again at 80 °C for 5 min to form a bilayer of positive tone resist to facilitate lift-off. The samples were patterned with a hexagonal array of 100 nm diameter circles on a 700 nm pitch, using direct electron-beam lithography (VISTEC electron-beam pattern generator (EBPG) 5000+) with an acceleration voltage of 100 keV and a current of 5 nA. After electron-beam writing, the pattern was developed in a 1:3 MIBK (methyl isobutyl ketone):isopropanol for 60 s at room temperature, resulting in a hexagonal array of 100 nm diameter holes with a 700 nm pitch in the PMMA layers. A 200 nm layer of Cr was evaporated over these samples (rate 1 A·s<sup>-1</sup> at 10<sup>-6</sup> Torr), and lift-off was performed in acetone, leaving a hexagonal array of Cr that served as a hard mask for TiO<sub>2</sub> dry etching. Dry etching was then conducted using an Oxford Instruments Plasma Lab System 100 ICP-RIE by using SF<sub>6</sub> / C<sub>4</sub>F<sub>8</sub> etching chemistry, in which SF<sub>6</sub> was the etching gas and C<sub>4</sub>F<sub>8</sub> was the passivating gas. Etching was performed at a capacitively coupled power of 150 W, an inductively coupled power of 2500 W, a SF<sub>6</sub> / C<sub>4</sub>F<sub>8</sub> gas ratio of 23.5 sccm / 40 sccm, a chamber pressure of 7 mTorr, and a table temperature of 0 °C for 15 min.

Electrodes were prepared from the n<sup>+</sup>p-Si samples with etched TiO<sub>2</sub> cones by first cleaving the samples to remove the edges, thus avoiding shorts due to doped layers. In-Ga eutectic was applied on the back side of the samples to form an ohmic contact to the p<sup>+</sup>n-Si homojunction. Ag paste

(Ted Pella) was used to attach a Sn-plated Cu wire to the In-Ga on the back side of the sample. The wire was run through a glass tube, and the samples were sealed to the glass tube using epoxy (Loctite 9460), and annealed at 80 °C for ~ 6 h. The active area of the electrodes was determined using a high-resolution image taken using a commercial scanner and image-processing software (ImageJ). Typical electrode areas were ~ 0.04 cm<sup>2</sup>.

The samples were then dipped in buffered HF (40% NH<sub>4</sub>F to 49% HF volume ratio 6:1) for 10 s to remove the remaining SiO<sub>2</sub> between the TiO<sub>2</sub> cones and to fully remove the Cr mask. The Ni layer was subsequently electrodeposited on the areas of the surface of the p<sup>+</sup>n-Si between the TiO<sub>2</sub> nanocones using a commercially available Ni plating solution (Clean Earth Nickel Mirror, Grobet USA) at a potential of -0.956 V vs Ag /AgCl (using a Biologic SP-200 potentiostat) until ~ 300 mC cm<sup>-2</sup> of cathodic charge was passed.

An illustration of the process flow for fabrication of the desired structures is shown in Supplementary information Fig. S5.

#### *Fabrication of an array of holes in a Ni layer on p<sup>+</sup>n-Si*

Electron-beam evaporation was used to deposit a layer of Ni on p<sup>+</sup>n-Si samples. The samples were then covered with ZEP 520A by spin-coating at 4000 rpm for 60 s and were baked at 180 °C for 3 min. A hexagonal array of circles 500 nm in diameter with a 700 nm pitch was written onto the samples by direct electron-beam lithography using an acceleration voltage of 100 keV and a current of 50 nA. The pattern was then developed by immersing the samples in a ZED N50 solution for 90 s. The patterned resist was used as a mask for ICP-RIE etching of the Ni film. Etching was performed using the following parameters: 4 mTorr, 600 W ICP forward power, 150 W RF forward power, 20 °C, 30 sccm Ar. The final removal of ZEP 520A was performed using remover PG.

#### *Photoelectrochemical oxygen-evolution reaction (OER)*

A three-necked glass cell with a quartz window was used as a vessel for this experiment. The OER was performed in aqueous 1.0 M KOH (Sigma-Aldrich) using a three-electrode setup, with a saturated calomel electrode (SCE) as the reference electrode, a carbon electrode as the counter electrode, and the p<sup>+</sup>n-Si sample with TiO<sub>2</sub> cones and Ni as the working electrode. Measurements were conducted under simulated sunlight (Oriel Instruments Solar Simulator equipped with a 1000

W Mercury Xenon lamp calibrated to  $100 \text{ mW cm}^{-2}$  (AM1.5) illumination using a Si photodiode). For current-density versus voltage ( $J-V$ ) measurements, the voltage was swept at a scan rate of  $50 \text{ mV s}^{-1}$  from -0.5 V to 1.5 V vs SCE.

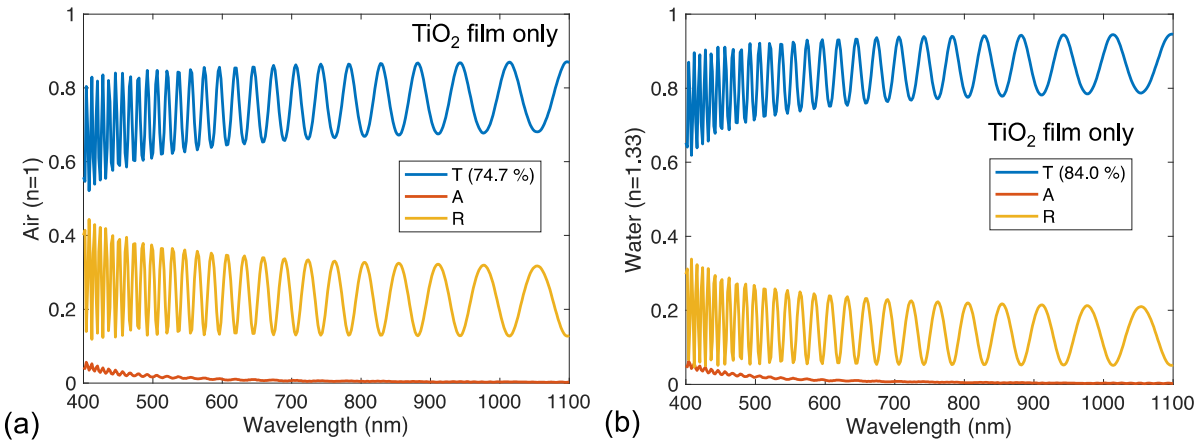
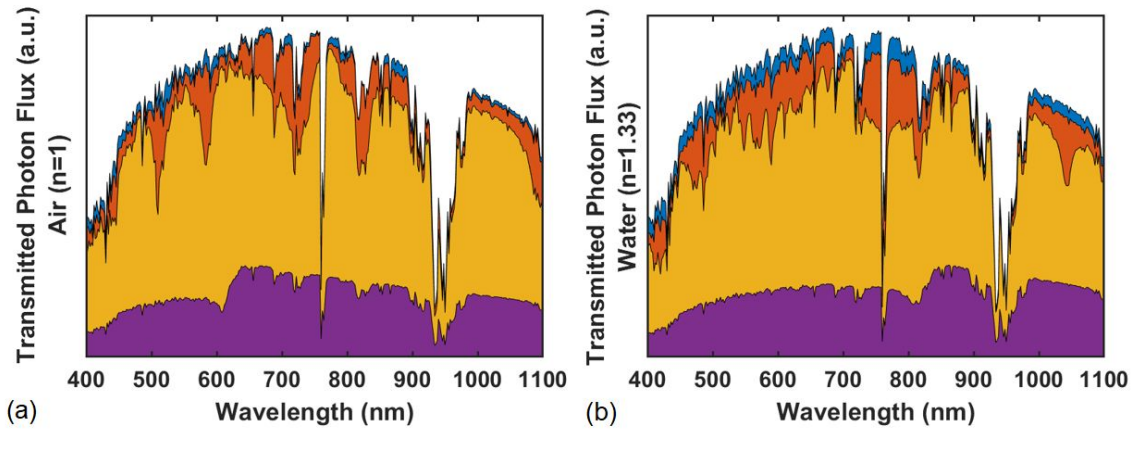


**Figure S1:** Simulated transmission (T), absorption (A), and reflection (R) spectra of the  $\text{TiO}_2$  film with thickness of  $2.3 \mu\text{m}$ . (a) plot the spectra in air (b) plot the spectra in water.



■ AM 1.5G ■ Nanocones on Si ■ Nanocones on Si with Ni ■ Ni hole array on Si

**Figure S2.** Area plot of simulated transmitted spectral photon flux in air and water for the three structures in Figure 1. Blue represents the AM 1.5G spectral photon flux. Orange, yellow, and purple depict the transmitted spectral photon flux into Si for: nanocones on Si, nanocones with Ni on Si, and Ni hole array on Si, respectively.

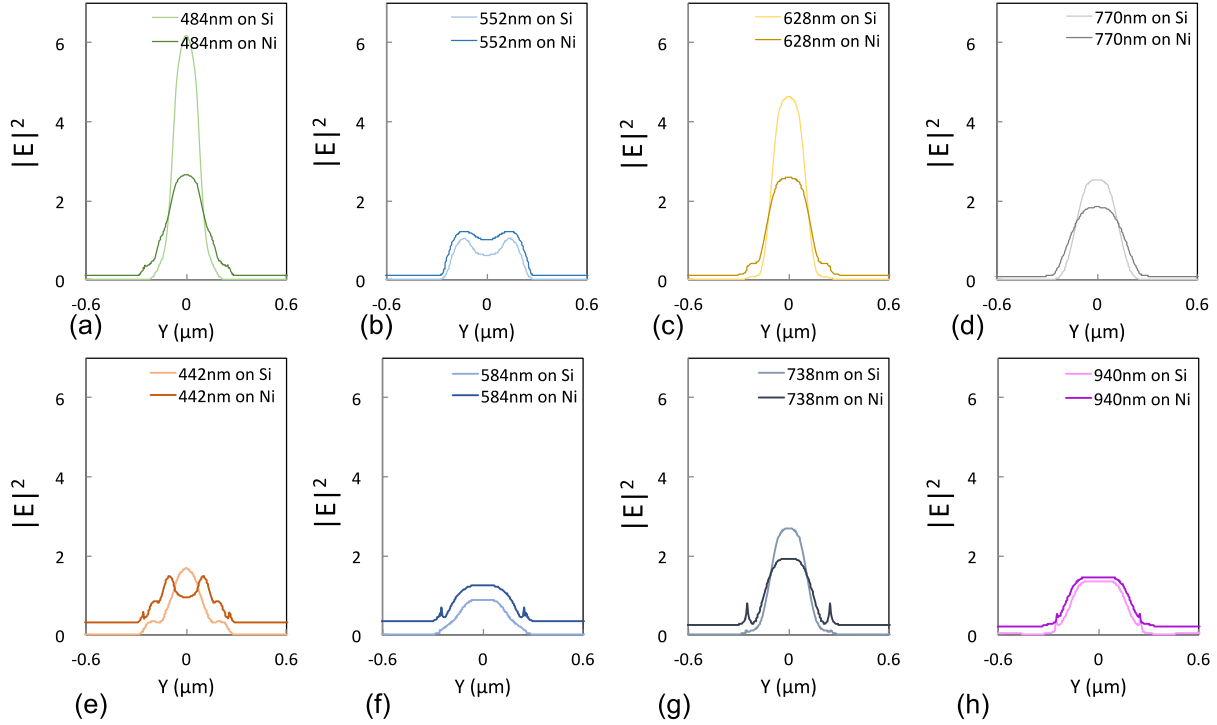


**Figure S3:** Transmitted light intensities  $|E|^2$  versus  $Y(\mu\text{m})$  at interfaces of Si/Ni (indicated as on Si) and Ni/air (indicated as on Ni). (a-d) Profiles for wavelengths of 484 nm, 552 nm, 628 nm, and 770 nm, respectively, which correspond to the maxima in the transmission spectra shown in Figure 2b. (e-h) Profiles for wavelengths of 442 nm, 584 nm, 738 nm, and 940 nm, respectively, which correspond to minima in the transmission spectrum in Figure 2b.

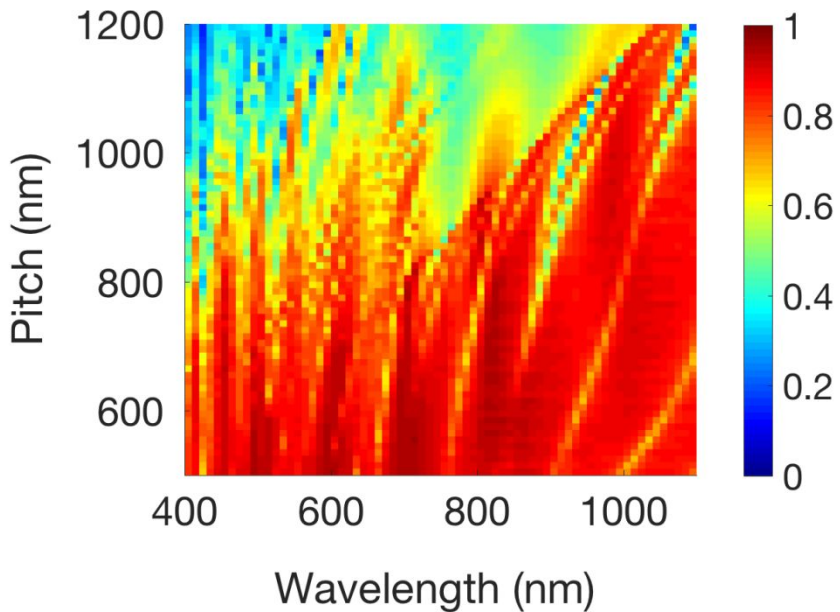


**Figure S4.** Dimension variation effect of Ni film on transmission to Si through  $\text{TiO}_2$  nanocone waveguides in air. Hexagonal array (variant pitches) of  $2.5\ \mu\text{m}$  tall cones with a  $200\ \text{nm}$  base radius and a  $50\ \text{nm}$  tip with a  $200\ \text{nm}$  radius Ni hole array.

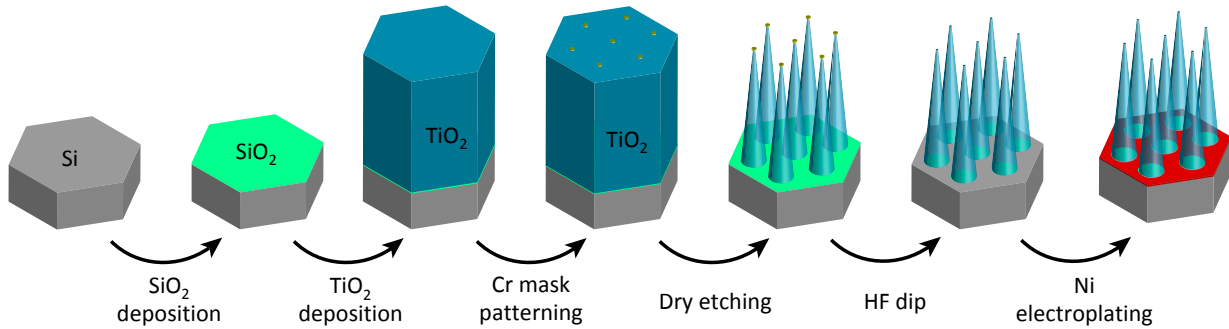


**Figure S5.** Process flow diagram for fabrication of Si photoanodes with  $\text{TiO}_2$  nanocones and Ni catalysts.

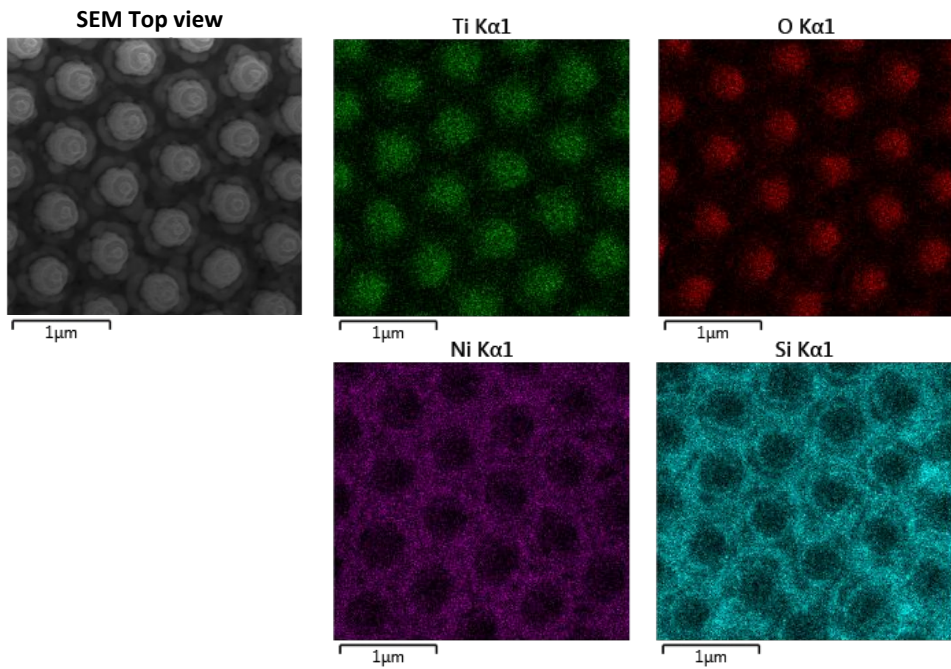


**Figure S6:** EDS mappings of elements Ti, O, Ni, Si with top view of the Ni/TiO<sub>2</sub> nanocones/p<sup>+</sup>n-Si sample.

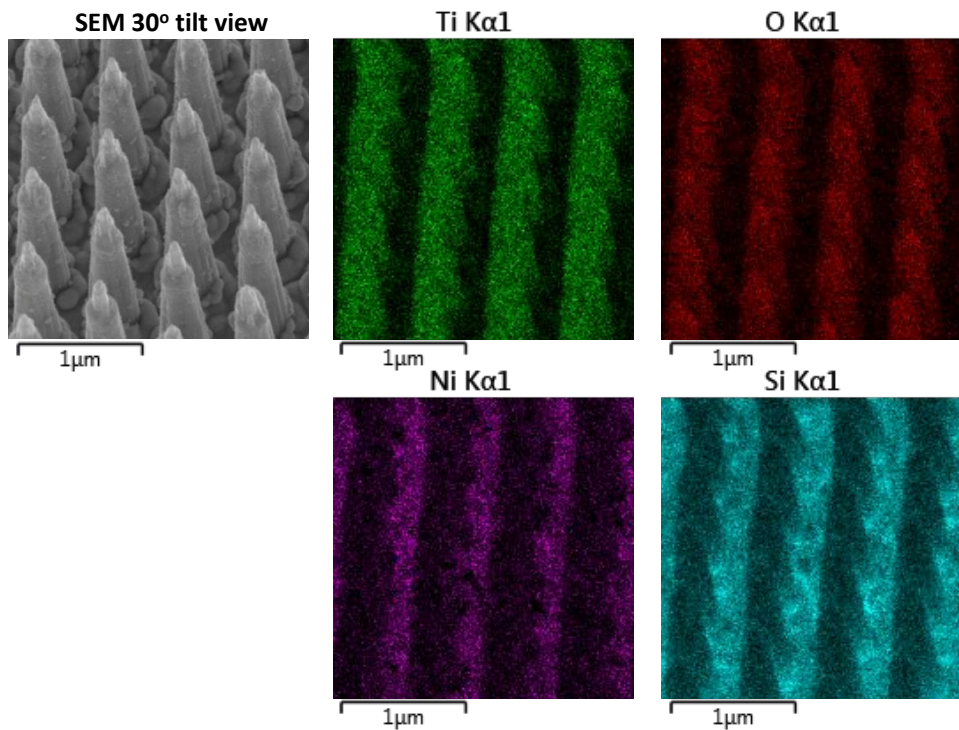


**Figure S7:** EDS mappings of elements Ti, O, Ni, Si with 30° tilt view of the Ni/TiO<sub>2</sub> nanocones/p<sup>+</sup>n-Si sample.

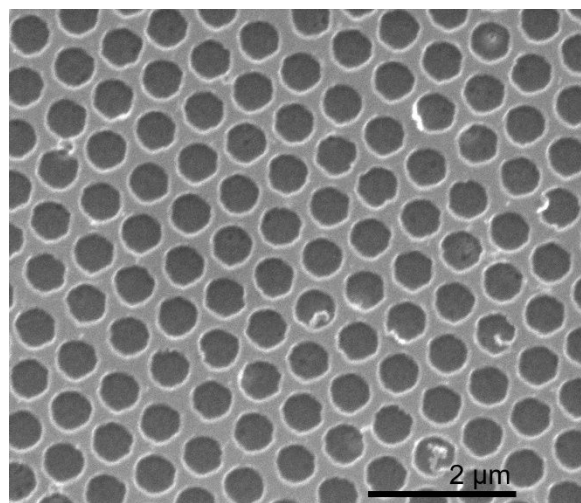


**Figure S8.** SEM image of the Ni hole array fabricated via electron-beam patterning and dry etching of a 50 nm thick Ni layer. The average diameter of the holes was ~ 500 nm.

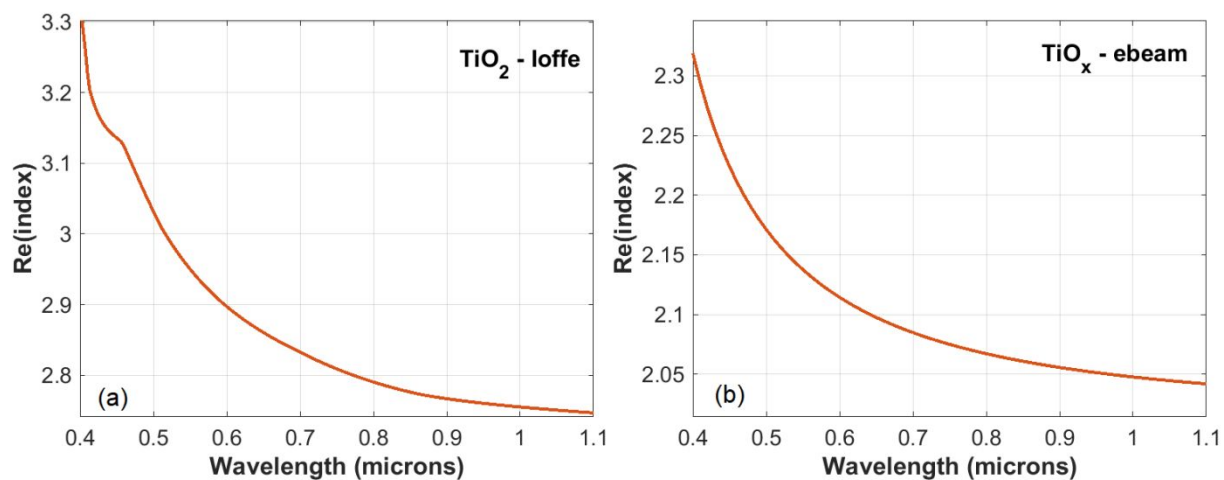


**Figure S9.** Real component of the refractive index for (a) an ideal rutile  $\text{TiO}_2$  standard, and (b) measured for a sample of electron-beam-evaporated amorphous  $\text{TiO}_2$ .